T-dependent RMF Model Applied to Ternary Fission Studies

C. Kokila*, C. Karthika and M. Balasubramaniam

Department of Physics, Bharathiar University, Coimbatore, Tamil Nadu – 641046, India

*ckokilaphysics@gmail.com (Corresponding Author)

ARTICLE INFORMATION

ABSTRACT

Ternary decay is comparatively a rare phenomenon. The yield distribution for the thermal neutron-induced fission of ^{236}U was investigated within the Temperature-dependent Relativistic Mean Field (TRMF) approach and statistical theory. Binding energy obtained from TRMF for the ground state and at a specific temperature is used to evaluate the fragment excitation energy, which is needed to calculate the nuclear level density. Using the ternary convolution, the yield for α-accompanied fission of ^{236}U* is calculated. Initial results are presented which shows a maximum yield for the fragment pair Tc + Ag +α. Further, the ternary pre-existence probability for the spontaneous fission of ^{236}U was studied considering fixed third fragments of α,^{10}Be and ^{14}C using the area of the overlapping region. No significant change in the yield distribution was observed when fragment deformations are considered. However, the heavy group for the probable pair remains as ^{132}Sn with a change in mass number of the lighter fragment.

1. Introduction

The unstable nuclei undergo radioactive decay by emitting radiations such as α, β and γ. Nuclear fission is another important process in which the nucleus splits into particles spontaneously or through induced processes along with the release of energy. When the excitation energy of the fragments is smaller, no neutrons are emitted and the phenomenon is known as cold fission. In such processes, one of the fragments was found to be associated with the closed-shell nuclei.

Ternary fission is an exotic decay mode in which the parent system splits into three fragments, and can be used as a probe to study the nuclear structure information. α accompanied fission is mostly observed as the light charged particle accompanied fission with its energy spectrum from 6 to 40 MeV. The size of the third particle varies from neutron to the case of true ternary fission in which the three fission fragments are of equal mass. Light particles such as H, Li, Be, and C were also observed in the spontaneous fission of various parent systems.

The experimental investigation [1] for the neutron-induced fission of ^{235}U indicated the presence of one α-particle per 250 fissions. Further Tsien et al., [2] studied the mass and kinetic energy of fission fragments in the tripartition of ^{235}U. Mostly the third particle was observed perpendicular to the other two heavier masses. In addition, the authors reported the quadripartition of the uranium nucleus, with the frequency of occurrence as 1/3000 that of bipartition. The α-particle accompanied and binary fission of ^{235}U was experimentally investigated by Asghar et al., [3] and have observed a similar distribution of fragment kinetic energy for the two fission modes. Furthermore, the mass distributions obtained for the binary and α-accompanied fission are in similar form with a narrow distribution for the latter case. The relative yields for ^{3}H, ^{3}He, and ^{4}He and their energy distributions were studied for thermal neutron-induced fission of ^{235}U [4-6].

To understand the ternary decay mechanism, various theoretical models have been developed. The ternary decay of heavy nuclei was studied using the Three Cluster Model (TCM) proposed by Manimaran and Balasubramaniam [7-10]. Vijayaraghavan et al. [11] also used the potential energy surface to study the fragment arrangements for the ternary fragmentation of ^{252}Cf. One of the authors has studied the binary [12] and ternary mass distribution [13] for the thermal neutron-induced fission of ^{236}U within the dynamical and scission point model respectively.

A brief account of yield calculation for the ternary decay of ^{236}U using the relativistic mean-field approach and statistical theory is described in the next section. Following that, the ternary pre-existence probability estimation of ^{236}U using the area of the overlapping region will be presented. In the subsequent sections, the preliminary results obtained by the two approaches are presented, followed by a summary.

2. Methodology

The ternary decay of thermal neutron-induced fission of ^{236}U is considered with α-particle as the fixed third fragment. The possible mass fragmentations are generated by comparing with the mass table [14] along with the constraint $A_1 \geq A_2 \geq A_3$ and $A = A_1 + A_2 + A_3$. A_3 is the smallest fragment, taken as fixed and is considered here as α-particle. The interaction potential is calculated using Eq. (1) assuming deformed fragments (A_2 and A_1) in the equatorial arrangement. It is given by,

$$V = \sum_{i=1}^{3} BE_i(T) + \sum_{i=1}^{3}\sum_{j>i}^{3}\left[V_{coul}^{ij}(\beta,T) + V_{nucl}^{ij}(\beta,T)\right].$$
(1)

The temperature-dependent binding energy, $BE_i(T)$ is calculated using the relativistic mean-field (RMF) formalism which is briefly described below. Here constant temperature corresponding to the compound nucleus (CN) excitation energy is used. To evaluate the Coulomb and nuclear potential, the quadrupole deformation values obtained from the RMF approach is used rather than using the experimental data. As a preliminary calculation, we have restricted to only the quadrupole deformation values. The Coulomb potential is defined as:

$$V_{coul}^{12}(\beta,T) = V_{C_0}\left\{1 + V_{C_1} + V_{C_2} + V_{C_3} + V_{C_4}\right\}.$$
(2)

The terms involved are defined in Refs. [15,16]. The radii of deformed fragments are calculated with $R_i(\theta_i) = R_{0i}\left[1 + \beta_i Y_{20}(\theta_i)\right]$, where, $R_{0i}(T) = \left[1.28A_i^{1/3} - 0.76 + 0.8A_i^{-1/3}\right](1 + 0.0007T^2)$, and $R_t = R_1 + R_2$ is the touching point. The nuclear potential is given by,

$$V_{nucl}^{12}(\beta,T) \approx S(\beta_1,\beta_2)V_{N0}(T),$$
(3)

$S(\beta_1,\beta_2)$ gives the strength of nuclear interaction and the associated terms are described in Refs. [15, 17]. The proximity potential for the spherical fragments [18] is given by,

$$V_{N0}(T) = 4\pi\bar{R}\gamma b(T)\phi\left[s(T)\right],$$
(4)

with $\bar{R}, \gamma, b(T)$ and $\phi\left[s(T)\right]$ as the inverse of the root-mean-square radius, nuclear surface energy term, surface width, and universal function respectively.

The obtained fragmentation potential is then minimized for the charge number and further, we have restricted the input mass fragment window from $A_2 = 60$.

2.1. Relativistic Mean-Field Theory

The phenomenological description of ground-state properties of nuclei is successfully established using relativistic mean-field calculations. Interactions between nucleons are assumed to occur through mesonic fields. The relativistic description considers the spin-orbit interaction and the shell model properties of the nuclei. It is possible to calculate the nuclear binding energies, quadrupole deformation, r.m.s. radii, and matter density distribution within the RMF approach.

RMF Formalism

Nucleons are considered as Dirac spinors interacting among themselves by the exchange of mesons. The relativistic Lagrangian density [19, 20] for the nucleon-meson interaction is given as:

$$\begin{aligned}
\mathcal{L} &= \bar{\psi}_1\left\{i\gamma^\mu\partial_\mu - M\right\}\psi_i + \frac{1}{2}\partial^\mu\sigma\partial_\mu\sigma - \frac{1}{2}m_\sigma^2\sigma^2 \\
&\quad - \frac{1}{3}g_2\sigma^3 - \frac{1}{4}g_3\sigma^4 - g_\sigma\bar{\psi}_1\psi_i\sigma - \frac{1}{4}\Omega^{\mu\nu}\Omega_{\mu\nu} \\
&\quad + \frac{1}{2}m_\omega^2 V^\mu V_\mu - g_\omega\bar{\psi}_1\gamma^\mu\psi_i V_\mu - \frac{1}{4}\vec{B}^{\mu\nu}.\vec{B}_{\mu\nu} \\
&\quad + \frac{1}{2}m_\rho^2\vec{R}^\mu.\vec{R}_\mu - g_\rho\bar{\psi}_1\gamma^\mu\vec{\tau}\psi_i.\vec{R}^\mu \\
&\quad - \frac{1}{4}F^{\mu\nu}F_{\mu\nu} - e\bar{\psi}_1\gamma^\mu\frac{(1-\tau_3)}{2}\psi_i A_\mu.
\end{aligned}$$
(5)

ψ_i is the single-particle Dirac spinor, the masses and the field tensors of σ, ω and ρ mesons are respectively denoted as m_σ, m_ω and m_ρ and σ, V_μ and $\vec{R}_\mu. g_\sigma, g_\omega, g_\rho$ and $\frac{e^2}{4\pi}$ are the coupling constants for the σ, ω, ρ mesons and the photon fields respectively.

The equations of motion can be obtained from the classical variational principle. Dirac equation for the nucleons [Eq. (6)] and the Klein-Gordon equations [Eqs. (7a)-(7d)] for the mesons are obtained. They are given by:

$$\left\{-i\alpha.\nabla + V(r) + \beta\left[M + S(r)\right]\right\}\psi_i = \varepsilon_i\psi_i,$$
(6)

$$\left\{-\Delta + m_\sigma^2\right\}\sigma(r) = -g_\sigma\rho_s(r) - g_2\sigma^2(r) - g_3\sigma^3(r),$$
(7a)

$$\left\{-\Delta + m_\omega^2\right\}\omega_0(r) = g_\omega\rho_v(r),$$
(7b)

$$\left\{-\Delta + m_\rho^2\right\}\rho_0(r) = g_\rho\rho_3(r),$$
(7c)
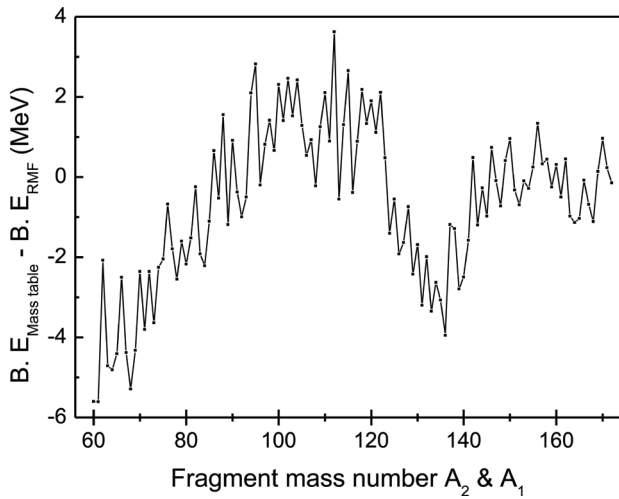
$$-\Delta A_0(r) = e\rho_c(r).$$
(7d)

Figure 1: Difference between binding energy calculated from TRMF and experimental value [14].

The nucleon and meson equations form a set of coupled equations and are solved iteratively. The total energy is given by,

$$E(T) = \sum_i \varepsilon_i n_i + E_\sigma + E_{\sigma NL} + E_\omega \\ + E_\rho + E_C + E_{pair} + E_{c.m.} - AM. \quad (8)$$

ε_i is the single-particle energy, n_i is the occupation probability, $E_\sigma, E_\omega, E_\rho$ and E_C are the contributions of the mesons fields and the Coulomb field. E_{pair} and $E_{c.m.}$ are the pairing energy and centre of mass correction. Pairing energy is,

$$E_{pair} = -G \left(\sum_{i>0} u_i v_i \right)^2,$$

G is the pairing force constant and u_i^2 and v_i^2 are the occupation probabilities. Temperature is included in the partial occupancies as:

$$n_i = v_i^2 = \frac{1}{2} \left[1 - \frac{\varepsilon_i - \lambda}{\tilde{\varepsilon}_i} \left[1 - 2f(\tilde{\varepsilon}_i, T) \right] \right],$$

with $f(\tilde{\varepsilon}_i, T) = \frac{1}{1 + e^{\tilde{\varepsilon}_i / T}}$ representing the Fermi-Dirac distribution function and $\tilde{\varepsilon}_i = \sqrt{(\varepsilon_i - \lambda)^2 + \Delta^2}$. The chemical potential λ for neutrons and protons is obtained from particle number conservation equations. Here we have calculated the binding energy of the nuclei using TRMF formalism.

The difference between binding energies obtained from TRMF formalism and experimental values is shown in Fig. (1). The binding energies obtained by the TRMF approach is found to be comparable with the predicted experimental values for the considered mass range. Hence,

this model may be appropriate to evaluate the binding energy at the ground and excited state.

2.2. Statistical Theory

The statistical theory considers nucleons as non-interacting fermions [21]. The Fermi-Dirac occupation probability can be used to estimate the energy of the nucleus. The level density of the system is:

$$\rho_i(E_i^*) = \frac{1}{12} \left(\frac{\pi^2}{a_i} \right)^{1/4} E_i^{*(-5/4)} \exp\left(2\sqrt{a_i E_i^*} \right), \quad (9)$$

where a_i is the level density parameter and is given as $a_i = E_i^* / T^2$. The relative fission probability at the scission point is proportional to the folded level density of quantum states of the fission fragments.

$$P(A_i, Z_i) \propto \rho_{123},$$

The ternary convoluted level density ρ_{123} [22, 23] is given by,

$$\rho_{123}(A_j, Z_j, E^*) = \int_0^{E^*} \rho_1(A_1, Z_1, E_1^*) \\ \times \left[\int_0^{E^*} \int_0^{E^*} \Pi_{i=2}^3 \rho_i(A_i, Z_i, E_i^*) \right. \\ \left. \delta \left[E_2^* + E_3^* - (E^* - E_1^*) \right] dE_i^* \right] dE_1^*,$$

where $j = 1, 2$ and 3. E_i^* is the excitation energy of fragment $i (= 1, 2$ and 3). For the minimized cases, the excitation energy of the fragments are evaluated as:

$$E_i^* = BE_i(T) - BE_i(T = 0), \quad (10)$$

with binding energy values obtained from TRMF formalism. The ternary fission yield is considered as the ratio between the probability of a given fragmentation and the sum of probabilities of all possible ternary fragmentations.

$$Y(A_i, Z_i) = \frac{P(A_i, Z_i)}{\sum P(A_i, Z_i)}. \quad (11)$$

2.3. Ternary Pre-existence Probability

According to Gamow's model, the preformation probability or the spectroscopic factor gives a measure of formation probability of fission fragments within the CN. Different approaches were developed to account for the fission process and to determine the preformation probabilities of nuclei.

Within the fission model, preformation probability was considered as the penetrability of the prescission part of the barrier. Two approaches were used for the preformation probability estimation. They are fission model, which was

developed based on the fission theory, and the preformed cluster-decay model (PCM) [24, 25] based on the collective model picture. Prescission and postscission parts of the potential were considered in the fission model, whereas only the outer part is present in the PCM. Poenaru et al. [26] have estimated the preformation probability within the unified fission approach. The penetration probability of the inner part of the barrier or the overlapping potential is considered as the preformation probability. One of us has studied the complete binary decay of ^{56}Ni, ^{116}Ba, ^{226}Ra and ^{256}Fm within the Unified Fission Model (UFM)[27]. As an extension, we also reported the pre-existence probability for the spontaneous ternary fission of various Cf isotopes from ^{242}Cf to ^{256}Cf in steps of two mass units with different choices of third fragments [28, 29].

Fragmentation Potential – Overlapping Area

The spontaneous ternary fission of ^{236}U is considered assuming an equatorial arrangement of fragments. The possible fragmentations are generated with the constraint $A_1 \geq A_2 \geq A_3$ and $A = A_1 + A_2 + A_3$ and by comparing with the mass table [14]. The interaction potential assuming spherical and deformed fragments are computed similar to Eq. (1). The Coulomb and nuclear potential are obtained from Eq. (2) and Eq. (3) for the deformed fragments. For the spherical calculations, they are respectively defined as $V_{coul}^{ij} = \dfrac{z_i z_j e^2}{R_t(T)}$ and as in Eq. (4). The radii of the fragment A_i is given by:
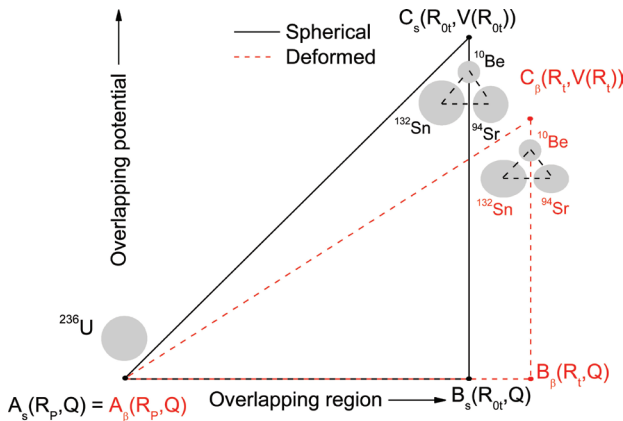

Figure 2: Overlapping region for a typical exit channel of ^{132}Sn + ^{94}Sr + ^{10}Be assuming spherical and deformed fragments.

$R_{0i}(A_i) = 1.2536 A_i^{1/3} - 0.80012 A_i^{-\frac{1}{3}} - 0.0021444 A_i^{-1}$. The scission point is taken at $R_{0ij} = R_{0i} + R_{0j} + \Delta R$. ΔR is the distance between the surfaces of two fragments and is taken as 1fm in the present calculation. For the charge minimized combinations, Q-values are calculated using experimental

masses. A typical overlapping region is shown in Fig. (2) for the exit channel of ^{132}Sn + ^{94}Sr + ^{10}Be assuming spherical and deformed fragments. The dotted line corresponds to the overlapping region assuming deformed fragments and the solid line depicts the overlapping region assuming spherical fragments. Here the overlapping region can be approximated as a triangle of base $R_{0t} - R_p$ fm and height $V(R_{0t}) - Q$ MeV and as $R_t - R_p$ fm and $V(R_t) - Q$ MeV respectively for spherical and deformed fragments. R_p is the radius of the parent system, R_{0t} and R_t are respectively the scission point for spherical and deformed fragments. Thus, the area of the overlapping region can be calculated using the values of potential, Q and radius of the nuclei at the scission point. The area can be correlated with the pre-existence probability of fission fragments. The overlapping area for the spherical and deformed fragments is given respectively as,

$$Area = \frac{1}{2}\Big[R_P - \big(R_{01} + R_{02} + \Delta R\big)\Big]\Big[\sqrt{V\big(R_{0t}\big) - Q}\,\Big],$$

and,

$$Area = \frac{1}{2}\Big[R_P - \big(R_1 + R_2 + \Delta R\big)\Big]\Big[\sqrt{V\big(R_t\big) - Q}\,\Big],$$

Then similar to WKB approximation, the probability,

$$P_0^i = \exp\left\{-\frac{2}{\hbar}\big(Area\big)\sqrt{2\mu_i}\right\},$$

can be obtained for the exit channel i. μ_i is the reduced mass of the ternary system. The normalized pre-existence probability P_0 can be obtained as:
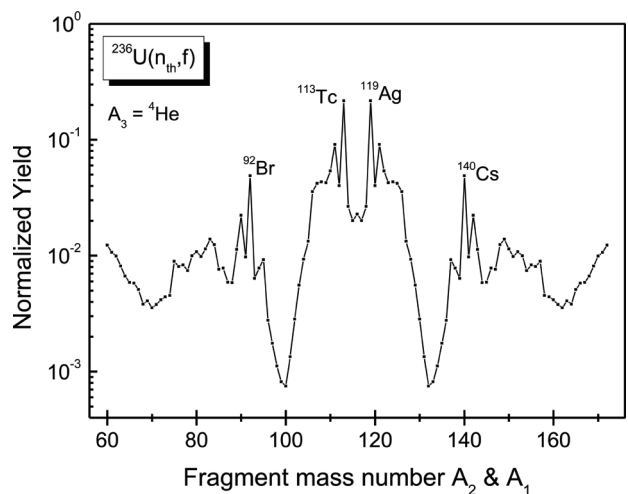
$$P_{ov}^i = \frac{P_0^i}{\sum_i P_0^i}.$$

Figure 3: Ternary yield distribution obtained from TRMF and Statistical theory for the thermal neutron induced fission of ^{236}U* considering α as the third particle.

3. Results and Discussion

3.1. Ternary Yield Distribution of $^{236}U^*$ using TRMF

The ternary yield distribution for the thermal neutron-induced fission of ^{236}U is studied within TRMF formalism and statistical theory. The nuclear level density was earlier [23,30] evaluated using single-particle energies obtained from the finite range droplet model (FRDM). The TRMF was already used to study the ternary decay of ^{252}Cf, ^{242}Pu and ^{236}U with $A_3 = {}^{48}Ca, {}^{20}O$ and ^{16}O using the level density approach [31] corresponding to temperatures T = 1, 2 and 3 MeV. Here, we studied the α-accompanied fission of ^{236}U considering the temperature as 0.51 MeV corresponding to the CN excitation energy of 6.5 MeV. The level densities calculated using TRMF formalism is used to evaluate the relative yield from Statistical Theory. For the possible mass fragmentations, the binding energies and quadrupole deformations of the nuclei at CN excitation energy and ground state are evaluated with the NL3 parameter set. The fragmentation potential is then calculated with the resultant deformation and binding energy values. For the charge minimized fragmentations, the excitation energy is evaluated using Eq. (10). Then the nuclear level density and the relative yield are evaluated using Eqs. (9) and (11) and the preliminary result obtained is shown in Fig. (3). Maximum yield is observed for the nearly symmetric breakup corresponding to the fragment pair Tc + Ag + α. Further, secondary maxima is observed for the fragmentation of Br + Cs + α. But, Sn + Zr was observed as the probable fragment pairs in the α-accompanied fission of $^{236}U^*$ [13]. It is planned to include the effect of channel temperature satisfying energy balance conditions within the TRMF formalism.

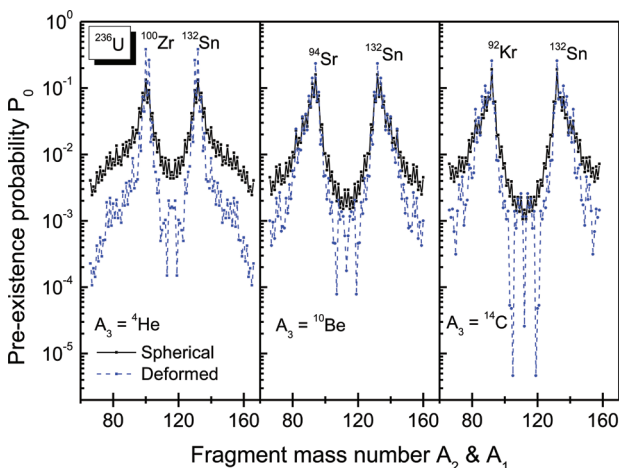**Figure 4:** Ternary pre-existence probability distribution for the spontaneous fission of ^{236}U considering α, ^{10}Be and ^{14}C as the third particles.

3.2. Ternary Yield Distribution of $^{236}U^*$ using Overlapping Area Approach

The area of the overlapping region may be approximated as a measure of pre-existence probability. The normalized pre-existence probability distribution for the spontaneous ternary decay of ^{236}U accompanied by fixed third fragments as ^4He, ^{10}Be and ^{14}C is shown in Fig. (4) assuming spherical and deformed fragments. The fragment pairs with maximum yield are also marked in the plot. The probable pairs are the same for spherical and deformed fragments. However, the heavier group remains as the closed-shell nucleus, ^{132}Sn for three choices of the third fragment with a corresponding shift in the light fragment mass number. A decrease in the yield values is observed when fragment deformations are considered except at the probable fragment pairs. In addition, with an increase in the mass number of the third fragment, there is a gradual shift from narrow distribution of P_0 to broader distribution.

Summary

Two approaches were used to study the ternary yield distribution for the α accompanied fission of ^{236}U. The ternary convolution was used in Statistical theory to obtain the relative yield using the binding energy of the ground and excited states derived via TRMF. Quadrupole deformation of the fragments from TRMF formalism was also used to choose the minimized fragmentations. Tc + Ag + α fragment pairs have the maximum yield. The pre-existence probability distribution for the α, ^{10}Be and ^{14}C accompanied spontaneous fission of ^{236}U was studied using an analytical method. The area of the overlapping region was correlated with the pre-existence probability of fragments. The fragment pairs corresponding to maximum yield remains the same for spherical and deformed fragments.

Reference

[1]   G. Farwell, E. Segrè and C. Wiegand, Phys. Rev. **71**, 327 (1947). https://doi.org/10.1103/PhysRev.71.327

[2] Tsien San-Tsiang, Ho Zah-Wei, L. Vigneron and R. Chastel, Nature **159**, 773 (1947). https://doi.org/10.1038/159773a0

[3] M. Asghar et al., Nucl. Phys. A **145**, 657 (1970). https://doi.org/10.1016/0375-9474(70)90446-X

[4] G. Kugler and W. B. Clarke, Phys. Rev. C **5**, 551 (1971). https://doi.org/10.1103/PhysRevC.5.551

[5] C. Wagemans, P. D'hondt, P. Schillebeeckx and R. Brissot, Phys. Rev. C **33**, 943 (1986). https://doi.org/10.1103/PhysRevC.33.943

[6] J. K. Hwang, Phys. Rev. C **61**, 047601 (2000). https://doi.org/10.1103/PhysRevC.61.047601

[7] K. Manimaran and M. Balasubramaniam, Phys. Rev. C. **79**, 024610 (2009). https://doi.org/10.1103/PhysRevC.79.024610

[8] K. Manimaran and M. Balasubramaniam, J. Phys. G: Nucl. Part. Phys. **37**, 045104 (2010). https://doi.org/10.1088/0954-3899/37/4/045104

[9] K. Manimaran and M. Balasubramaniam, Eur. Phys. J. A **45**, 293 (2010). https://doi.org/10.1140/epja/i2010-11000-7

[10] K. Manimaran and M. Balasubramaniam, Phys. Rev. C **83**, 034609 (2011). https://doi.org/10.1103/PhysRevC.83.034609

[11] K. R. Vijayaraghavan, M. Balasubramaniam and W. von Oertzen, Phys. Rev. C **90**, 024601 (2014). https://doi.org/10.1103/PhysRevC.90.024601

[12] C. Kokila and M. Balasubramaniam, Phys. Rev. C **100**, 034607 (2019). https://doi.org/10.1103/PhysRevC.100.034607

[13] C. Karthika and M. Balasubramaniam, Eur. Phys. J. A **55**, 59 (2019). https://doi.org/10.1140/epja/i2019-12729-y

[14] M. Wang et al., Chin. Phys. C **41**, 030003 (2017). https://doi.org/10.1088/1674-1137/41/3/030003

[15] C. Kokila and M. Balasubramaniam, Phys. Rev. C **101**, 014614 (2020). https://doi.org/10.1103/PhysRevC.101.014614

[16] V. Yu. Denisov and N. A. Pilipenko, Phys. Rev. C **76**, 014602 (2007). https://doi.org/10.1103/PhysRevC.76.014602

[17] V. Yu. Denisov, N. A. Pilipenko and I. Y. Sedykh, Phys. Rev. C **95**, 014605 (2017). https://doi.org/10.1103/PhysRevC.95.014605

[18] J. Błocki, J. Randrup, W. Swiatecki and C. F. Tsang, Ann. Phys. (NY) **105**, 427 (1977). https://doi.org/10.1016/0003-4916(77)90249-4

[19] Y. K. Gambhir, P. Ring and A. Thimet, Ann. Phys. **198**, 132 (1990). https://doi.org/10.1016/0003-4916(90)90330-Q

[20] S. K. Patra and C. R. Praharaj, Phys. Rev. C **44**, 2552 (1991). https://doi.org/10.1103/PhysRevC.44.2552

[21] P. Fong, Phys. Rev. C **2**, 735 (1970). https://doi.org/10.1103/PhysRevC.2.735

[22] A. J. Cole, *Fundamental and Applied Nuclear Physics Series – Statistical models for nuclear decay from evaporation to vaporization*, edited by R. R. Betts and W. Greiner (Institute of Physics Publishing, Bristol and Philadelphia, 2000). https://doi.org/10.1201/9781420033472

[23] M. T. Senthil Kannan and M. Balasubramaniam, Eur. Phys. J. A **53**, 164 (2017). https://doi.org/10.1140/epja/i2017-12355-9

[24] R. K. Gupta, W. Scheid and W. Greiner, J. Phys. G: Nucl. Part. Phys. **17**, 1731 (1991). https://doi.org/10.1088/0954-3899/17/11/018

[25] W. Greiner and R. K. Gupta, *Heavy Elements and Related New Phenomena* (World Scientific, Singapore, 1999). https://www.worldscientific.com/worldscibooks/10.1142/3664

[26] D. N. Poenaru and W. Greiner, Phys. Scr. **44**, 427 (1991). https://doi.org/10.1088/0031-8949/44/5/004

[27] N. S. Rajeswari, K. R. Vijayaraghavan and M. Balasubramaniam, Eur. Phys. J. A **47**, 126 (2011). https://doi.org/10.1140/epja/i2011-11126-0

[28] K. Manimaran, Ph. D. thesis, Department of Physics, Bharathiar University (2011).

[29] C. Kokila and M. Balasubramaniam, J. Phys. G: Nucl. Part. Phys. **48**, 025102 (2021). https://doi.org/10.1088/1361-6471/abcb5a

[30] M. Balasubramaniam, C. Karthikraj, S. Selvaraj and N. Arunachalam, Phys. Rev. C **90**, 054611 (2014). https://doi.org/10.1103/PhysRevC.90.054611

[31] M. T. Senthil Kannan, Bharat Kumar, M. Balasubramaniam, B. K. Agrawal and S. K. Patra, Phys. Rev. C **95**, 064613 (2017). https://doi.org/10.1103/PhysRevC.95.064613

Journal of Nuclear Physics, Material Sciences, Radiation and Applications